Open-ended coaxial probe for permittivity measurements to 125 GHz

Jon Martens

As the need for materials measurements at high frequencies increases in the areas of electronics, biology, chemistry, pharmacology, and other areas, convenient measurement tools could be of considerable value. One such tool, an open-ended coaxial probe, has been used successfully at lower microwave frequencies for many years. New V (1.85 mm) and W (1 mm)-connectorized probes, accompanied by simple software and a powerful VNA platform, allow measurements to 70 and 125 GHz, respectively, with very good repeatability and accuracy. While most often used for liquids, these probes can also work well on solids when the material is compliant enough and can even be used on certain multi-layer structures.

Introduction

The concept of this probe is pretty much in its name and much has been published on the structure (e.g., [1]-[6]). As shown in Fig. 1, the structure consists of a very planar termination of a coaxial line with an extended ground plane. A schematic diagram is shown in Fig. 2 to illustrate a cut-away view of the probe near the face. The fields fringe out from the aperture (illustrated schematically in Fig. 3) and interact with the material in question, thus altering the measured reflection coefficient. The upper frequency limit is generally set by the coaxial aperture size while the lower frequency limit is generally set by the probe body size relative to that aperture. For the V probe, operation down to ~100 MHz is possible while for the W probe, 500-900 MHz is a common minimum frequency. As will be discussed, the choice of calibration standards has some impact as well on this lower frequency limit.

1.85 mm connector; 70 GHz | **1 mm connector; 110 GHz (125 GHz)**

Figure 1. *V- and W- connectorized open-ended coaxial probes are shown here along with their maximum operating frequencies. The W-probe is normally quoted as operational to 125 GHz although this does require that the cable connected to it also operates to that frequency.*

For liquid measurement applications, an important property of the probe is relative imperviousness to contamination by the material under test as that would alter future measurements. These probes have been constructed with a glass bead interface sealed against the surrounding metal walls with an advanced process to prevent any ingress except in the most corrosive of environments.

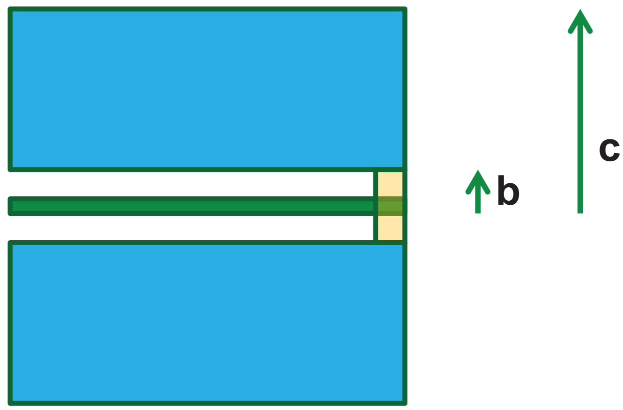

Figure 2. *The coaxial outer conductor (inner) radius 'b' is less than 0.2 mm for the W probe and is 0.6 mm for the V probe. The outer radius 'c' is 4.5 mm for both probes*

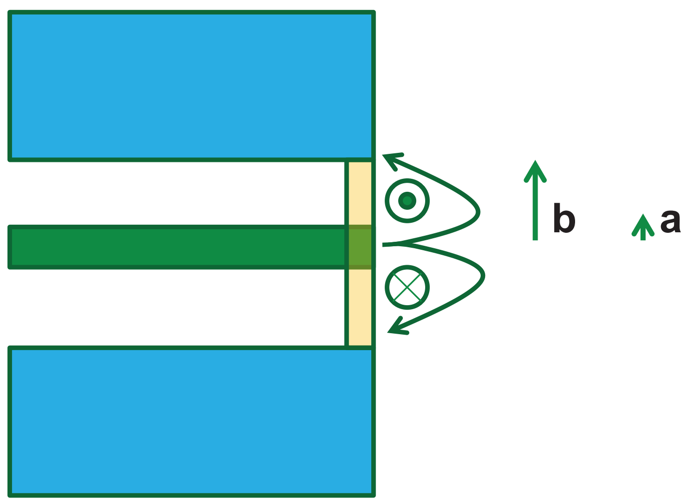

Figure 3. *Much of the behavior of the probe is governed by the aperture radii. The dimension 'a' is on the order of 0.12 mm for the V probe and 0.033 mm for the W probe.*

An example setup is shown in Fig. 4 where the probe (at the bottom of the picture) is connected via a W-connectorized coaxial cable to an Anritsu 3743A mm-wave module (part of a ME7838A 70 kHz-125 GHz broadband system). The whole module-cable-probe assembly is on a positioner rail so that the probe can be lowered into sample liquids without cable flex (which could add uncertainty) and without too much mechanical complication.

Figure 4. *An example setup is shown here where the W-probe is connected, via a flexible 1 mm cable (also operational to 125 GHz) to a 3743A mm-wave module. This module is, in turn, connected to a VNA as part of a ME7838A broadband system allowing measurements from 40 kHz to 125 GHz. Due to the probe lower frequency limit, a more common probe measurement range is, for example, 500 MHz-125 GHz.*

The reflection coefficient of an open probe (when left in air) is quite high as one would expect. A measurement, based on a calibration at the coaxial plane (OSL/SSS hybrid), is shown in Fig. 5 for a W probe. The magnitude is not 0 dB throughout due to some internal material loss and there is some ripple due to the fringing field capacitance interacting with the finite residual source match of the calibration (~30 dB in this case) but there are no resonances or other structure that might be indicative of far-field radiative losses. Data for the open and short (silver paint in this case) measured on a V probe (coaxial calibration again, OSL only this time) are also shown in Fig. 5 and again show relatively low loss and no evidence of radiative issues. In both cases, the losses are low enough and stable such that a calibration can readily correct for the probe behavior.

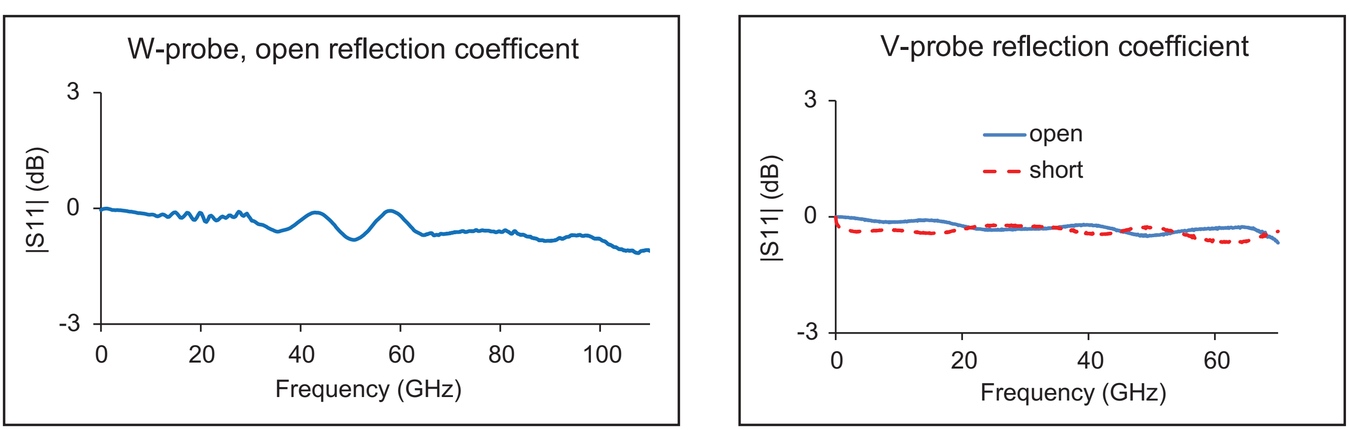

Figure 5. *The raw reflection coefficients of the probes (when left open, or in one case, when shorted) are shown here. The calibration for these measurements was done at the coaxial plane unlike what is done for the material measurements.*

Calibration methods

For a materials measurement, we wish to calibrate at the probe face. As with any one port reflection measurement, three calibration standards are required to be complete (e.g., [6]-[8]). Leaving the probe open is an easy ‘standard’ as the fringing fields in free-space are easily calculable. De-ionized (DI) water is a likely second candidate since its characteristics are well-known and a sample coming close to the semi-infinite space definition is usually practical to setup. Often a short is used as the third standard and this can be implemented in a number of ways including conductive silver paint (extremely repeatable but usually requires a solvent for removal), metal foams, or metal foil pressed up against the probe. The last item relies on capacitive coupling between the probe and the foil so the lower frequency may be limited and this limit will depend on the compliance of the foil as illustrated in Fig. 6.

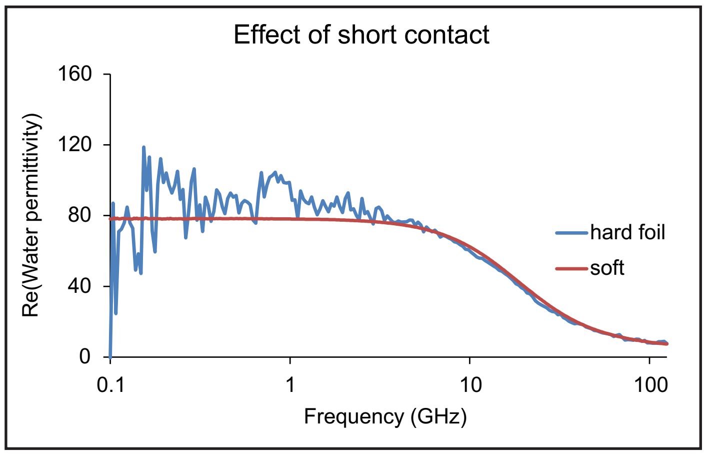

***Figure 6**. If using a metal foil as a short standard, the compliance of that material will have a large influence on the low frequency behavior. A softer foil is better and a conductive paint is even better.*

The use of other calibration materials is always possible assuming the reflection generated is sufficiently different from the other standards so there is no danger of a numerical singularity and the material is sufficiently well-understood. Some examples include:

– Open-short-DI water (standard approach)

– Open-short-methanol

– Open-short-ethanol

– Open-short-isopropanol

– Open-DI water-methanol

– Open-Short-soft PCB material (known from some other method)

– Open-short-standard rubber compound (known from some other method)

Example measurements: repeatability and accuracy

Repeatability of measurement and the accuracy of the extracted permittivity are always of interest. Some example measurements of isopropanol are shown in Fig. 7 using an open-DI water-silver paint-based calibration over 1-125 GHz using the W probe on a ME7838A broadband measurement system. Reference data below 32 GHz was available from the literature [9] and is included in the plot. Repeatability between the four trials was better than 0.2% on the real part and 1% on the imaginary part. The increase for the imaginary part repeatability and for deviations from the reference may be due to a variability of contamination in the sample as the atmosphere was not tightly controlled. The sample tested was about 20 µL in volume.

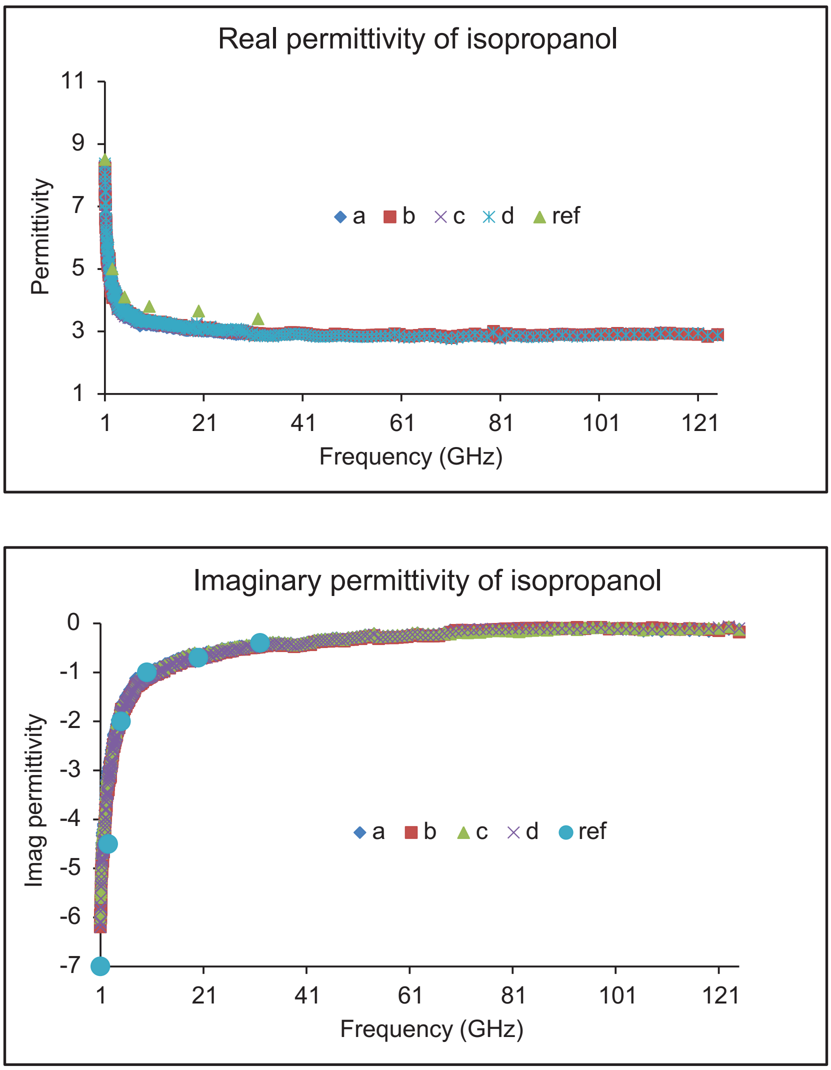

Figure 7. *Four separate measurements of the complex permittivity of isopropanol are shown here to illustrate repeatability. Reference values from the literature, at lower frequencies at least, are shown here for comparison.*

A slight variation on this experiment is to use physically different samples (and sample holders) to test a more practical repeatability and this result is shown in Fig. 8 for the V probe on a MS4647A 70 kHz-70 GHz VNA. With the V probe, data down to 100 MHz was available with decent repeatability.

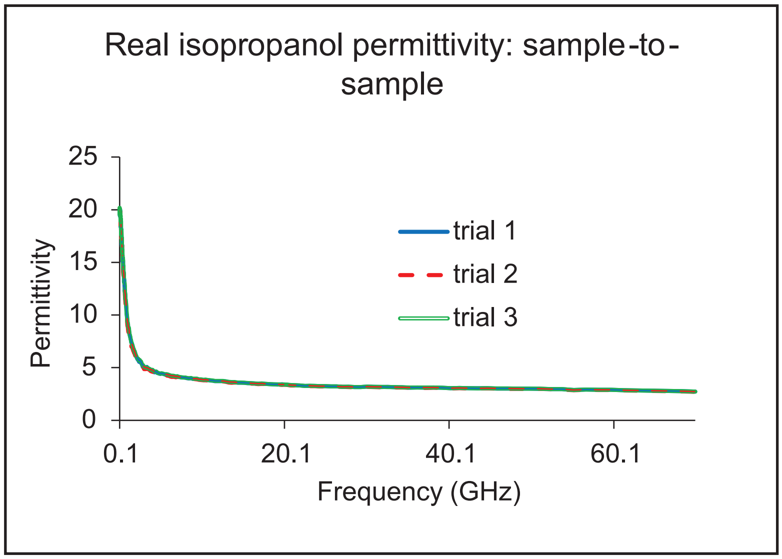

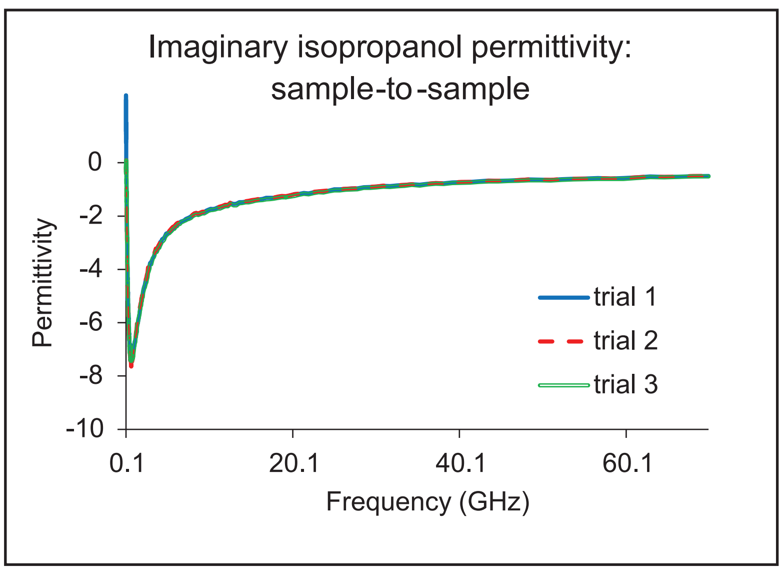

Figure 8. *As another measure of repeatability, three different samples of isopropanol (from the same lot) were measured using the V-probe.*

Yet another way of looking at repeatability is to perform multiple calibrations and measure the same sample. This measurement tests the ability to consistently apply the short (silver paint in this case), the ability to remove the short standard, and the consistency of the DI water standard. The results for isopropanol under these conditions are shown in Fig. 9 and show similar levels of repeatability on the real part and some degradation in the imaginary part. The latter is believed to be due to some contamination changes in the DI water standard and point to the importance of handling and environment control when pursuing the utmost in accuracy.

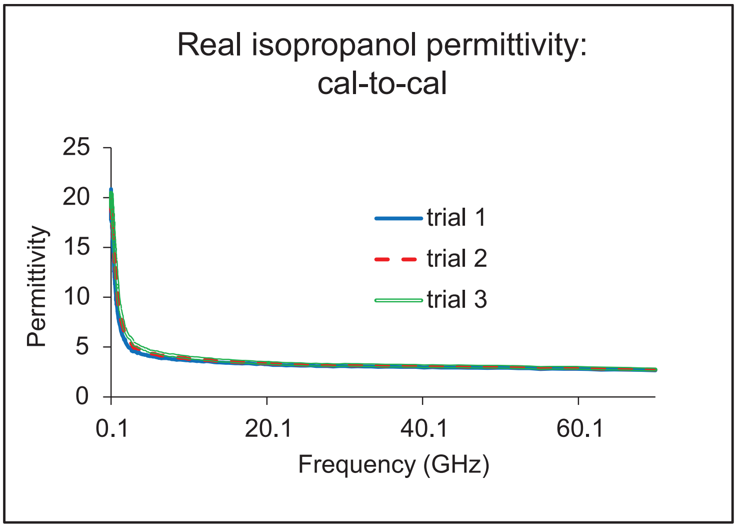

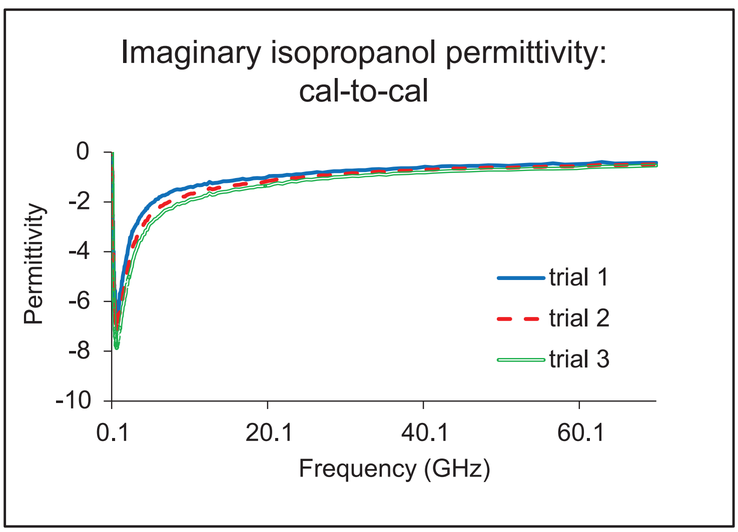

Figure 9. *A different type of repeatability is calibration-to-calibration. Here there is somewhat increased variability in part due to varying contamination of the DI water calibration standards.*

Software, computations and measurement execution

Once the calibration is complete, the calibrated reference plane for the reflection measurement has moved to the probe face. When the probe is connected to the MUT, it is now a matter of generating a permittivity that matches the measured reflection coefficient in a self-consistent way. In this particular case, a nonlinear curve fitting structure (courtesy Dr. Johannes Hunger, Max Planck Institute for Polymer Research) was implemented to find that permittivity in a robust fashion. This fitting process is then repeated at every frequency in the list.

To facilitate all of these steps, a simple software package (the Dielectric Probe Application) has been created that can run in the MS464XX VNA or can be run on an external PC (Windows 7 or XP, connected to the VNA via Ethernet for instrument control). The program sets up the VNA, performs the calibration and MUT measurement, and extracts complex permittivity. All MS464XX VNAs are supported including the broadband systems (e.g., ME7838A, 70 kHz-125 GHz). An example screen-shot is shown in Fig. 10 where a water sample is being measured over 5-110 GHz using a W probe. The real and imaginary parts of permittivity are plotted in the upper window and a Cole-Cole plot is available in the lower window. Direct reflection coefficient plotting is also available to help with multilayer structural analysis. Permittivity and reflection coefficient data can be output in a .txt file format (an example is shown in Fig. 11) and setups (including all instrument states and calibrations) can be saved and recalled.

In many cases, logarithmic sweeps and plots are required (particularly in broadband situations) and these are supported with independent controls. Port power is adjustable (including the use of step attenuator controls on a sub-dialog) which can be helpful for analyzing nonlinear materials. To help navigate the trade-off between trace noise and measurement time, IF bandwidth and sweep-by-sweep averaging (on a sub-dialog) are adjustable.

One may also notice an entry for water temperature in the dialog. Since the DI water is being used as a calibration standard and the permittivity of water is a strong function of temperature, a more complete model of water permittivity was employed [10]. It is valid over nominally 0 to 100 C and is based on a double time constant Debye model.

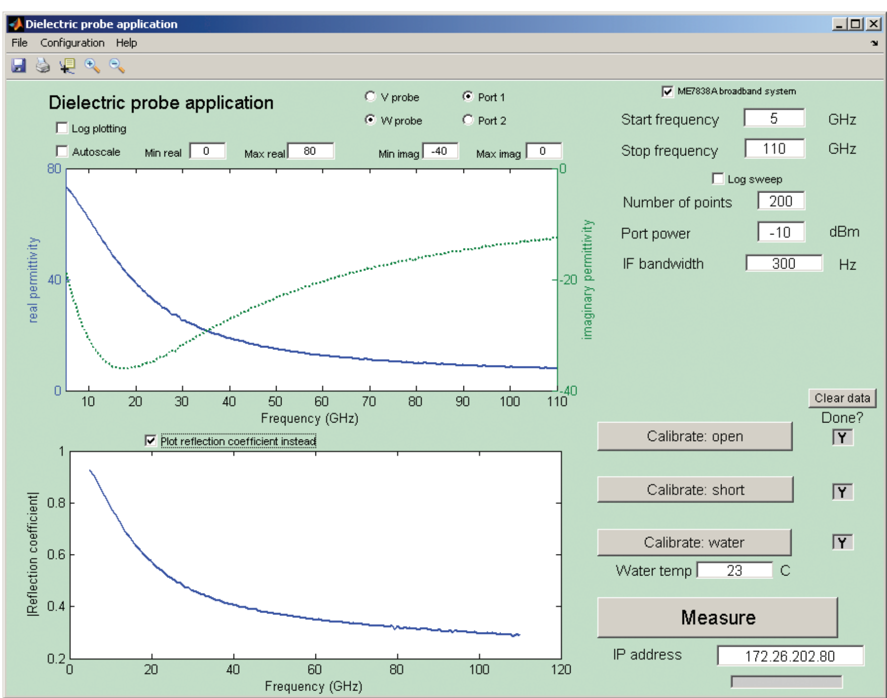

Figure 10. A screen-shot of a simple software package for performing the permittivity measurements is shown here. The software can run on the MS464XX VNA or can be run on an external PC.

When the software is run on the instrument itself, the loopback Ethernet IP address is employed (127.0.0.1) that allows communication entirely within the instrument. When the software is run on external PC, the instrument and the host PC must be on the same network (or accessible portions of a network) and the instrument IP address entered in the field provided.

!Freq (GHz)	real(eps)	imag(eps)	gamma(mag)	gamma (deg)
1	78.479	-2.4369	0.99802	-3.6518
1.0163	78.411	-2.5799	0.99787	-3.708
1.0328	78.849	-2.2321	0.99813	-3.7894
1.0496	78.4	-2.4789	0.99789	-3.8291
1.0667	78.55	-2.4019	0.99792	-3.8989
1.0841	78.197	-2.6614	0.99766	-3.9445
1.1017	78.335	-2.3761	0.99788	-4.0157
1.1197	78.073	-2.8537	0.99741	-4.0675
1.1379	78.187	-2.7144	0.9975	-4.1396
1.1564	78.437	-2.7302	0.99744	-4.2205
1.1753	78.161	-2.666	0.99746	-4.2741
1.1944	78.197	-2.6626	0.99742	-4.3456
1.2138	78.427	-2.4912	0.99755	-4.4293
1.2336	78.386	-2.9066	0.99709	-4.499
1.2537	77.979	-2.9661	0.99699	-4.5484
1.2741	77.576	-3.0611	0.99684	-4.5985
1.2948	77.917	-2.9902	0.99686	-4.6939
1.3159	78.207	-3.2491	0.99654	-4.788
1.3373	77.69	-3.4064	0.99631	-4.8337
1.3591	77.827	-3.3281	0.99634	-4.921
1.3812	78.05	-3.5598	0.99602	-5.0154
1.4037	77.729	-3.7013	0.99579	-5.076
1.4266	77.546	-3.7059	0.99572	-5.1464
1.4498	78.012	-4.0734	0.99522	-5.2615
1.4734	77.904	-4.0784	0.99514	-5.3397
1.4974	77.911	-4.3171	0.99477	-5.427
1.5217	77.742	-4.4924	0.99447	-5.5033

Figure 11. *An example portion of the text file format for saving data from the application is illustrated above. Real and imaginary parts of permittivity along with corrected reflection coefficient data (in linear magnitude and angle format; at the probe face reference plane) are stored for each frequency point. This example represents a log frequency sweep so the frequency steps are not equal in a linear sense.*

Uncertainties and other considerations

The basic uncertainty in the reflection coefficient measurement is determined by the agreement between the calibration standards and the models representing those standards, the trace noise, dynamic range and linearity of the VNA (e.g., [11]) and the repeatability of measurement of both the standards and the MUT. We have covered repeatability earlier and, in many cases, it still ends up being the dominant uncertainty element. In liquids cases with an adequate sample holder (greater than 5 aperture radii always available), this component should be no worse than 1% on real permittivity. Assuming IF bandwidth is set low enough for the power levels involved (100-300 Hz recommended for most conditions), the VNA-related uncertainty elements are normally contributing <<1 % of permittivity. The calibration standard agreement will, of course, vary with the standards chosen. The open model is generally very good unless the probe surface has been damaged and the DI water model has been validated many times but does make the assumption of no contaminants. The short standard, as has been discussed, can be more variable, in large part due to repeatability of that standard. Using a conductive paint generally keeps the standard uncertainty much less than that due to MUT contact repeatability.

The uncertainty on the imaginary part of permittivity is more difficult to assess but on high loss materials, it will tend to track the real permittivity uncertainty levels just discussed. Very low loss materials will show higher fractional uncertainties due to the increasing importance of trace noise and drift and the very high sensitivity of imaginary permittivity extractions to S-parameter uncertainty in these cases. Practical uncertainties may go to 10% or more for imaginary permittivities < 0.1.

As mentioned previously, one consideration is the depth or thickness of the sample and how closely it approximates the ‘infinite half-space’ condition. Measurements of an alcohol were done with the probe at various locations (Fig. 12) in the sample holder, labeled ‘a’ through ‘g’ in Fig. 13. The measurement at position ‘a’ was roughly 3 mm from the bottom of the container and 8 mm from the edges. The results show good consistency for measurements ‘a’ through ‘d’ with some variation starting to show up in ‘e’ through ‘g’ when the probe is getting within 5 coax radii of the bottom (<1 mm). The constraints on position become less stringent at higher frequencies as the fringing field range decreases.

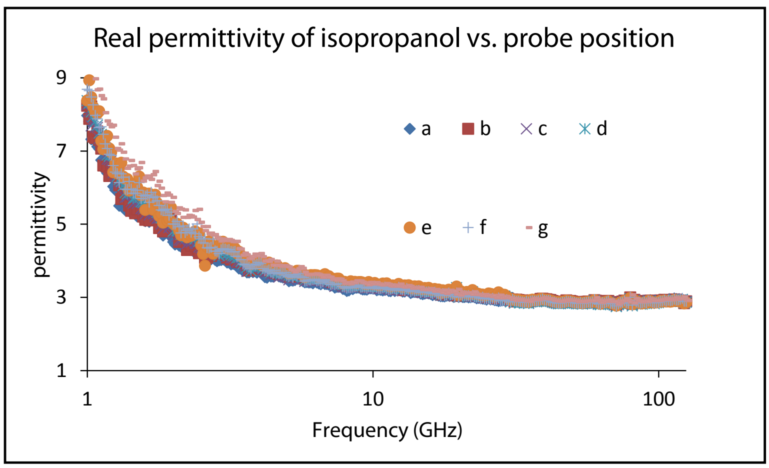

Figure 12. *The dependence of the measurement with the position of the probe relative to the container walls is illustrated here. Staying at least 5 coax radii from the edges generally will ensure decent results even at relatively low frequencies. The positions are described in Fig. 13.*

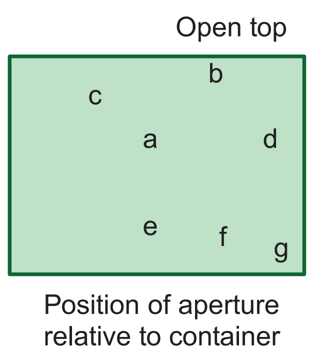

Figure 13. *The positions of the probe referenced in Fig. 12 are schematically illustrated here relative to the container walls and top.*

Softer solids can also be readily measured with the open coaxial probe (PCB material being one example). Harder materials are more difficult to analyze due to a possibly unpredictable air gap between the probe and the material but softer materials do not suffer from that issue. Often, however, these solid materials have a harder time meeting the ‘infinite half space’ requirement. While many techniques exist in the literature (e.g., [12]-[14]), for dealing with a variety of thin and multilayer stacks, we will only consider here the case of a thin dielectric backed by a conducting plane as suggested in Fig. 14.

__Figure 14.__ One measurement variant where the 'infinite half-space' condition is not met is shown here. A thin dielectric sheet that is backed by a conductor is to be measured. Here 'thin' means much less than the probe diameter and less than the aperture diameter.

In this case, the structure acts like a parallel-plate circular resonator [15] rather than a simple broadband reflection measuring setup. The structure will resonate at frequencies given by

$$f_{on} = \frac{c \cdot k_{on}}{2\pi r\sqrt{\varepsilon_r}}$$

Here, r is the radius of the probe and the k_{on} are the roots of the Bessel junction derivative J_0' (first few values are 3.8317, 7.0156, 10.1735, 13.3237 and 16.4706). By choosing to 'plot reflection coefficient instead' (of Cole-Cole) option in the software package, the resonant frequencies (f_{on}) will be obvious and one can quickly solve for permittivity. At non-resonant frequencies, the broadband processing can proceed but must be corrected for the finite thickness (e.g., [14], this correction is not currently part of the software package described earlier).

Summary

While open-ended coaxial probes have been used for materials measurements at lower frequencies for many years, the higher microwave and millimeter-wave ranges have not been explored nearly as often. V- and W- connectorized probes have been presented here along with an accompanying software package to make these measurements up to 125 GHz. The probe design allows convenient use with a variety of materials while having millimeter-wave properties consistent with repeatable calibrations. The measurements can be performed with very good repeatability and, with an appropriate calibration, the accuracy can also be very good under a variety of conditions.

References

1. E. C. Burdette, F. L. Cain, and J. Seals, "In vivo probe measurement technique for determining dielectric properties at VHF through microwave frequencies," IEEE Trans. Micr. Theory Tech., vol. 28, pp. 414-417, Apr. 1980.
2. C.-L. Li and K.-M. Chen, "Determination of electromagnetic properties of materials using flanged open-ended coaxial probe- full-wave analysis," IEEE Trans. Inst. Meas., vol. 44, pp. 19-27, Feb. 1995.
3. S. S. Stuchly, C. L. Sibbald, and J. M. Anderson, "A new aperture admittance model for open-ended waveguide," IEEE Trans. Micr. Theory Tech., vol. 42, pp. 192-198, Feb. 1994.
4. H. Levine and C. H. Papas, "Theory of the circular diffraction antenna," J. Appl. Phys., vol. 22, pp. 29- 43, 1951.
5. J. R. Mosig, J. –C. E. Besson, M. Gex.-Fabry, and F. E. Gardiol, "Reflection of an open-ended coaxial line and application to nondestructive measurements of materials," IEEE Trans. Instr. Meas., vol. 30, pp. 46- 51, Mar. 1981.
6. D. V. Blackham and R. D. Pollard, "An improved technique for permittivity measurements using a coaxial probe," IEEE Trans. Instr. Meas., vol. 46, pp. 1093-1099, Oct. 1997.
7. R. F. Bauer and P. Penfield, "De-embedding and unterminating," IEEE Trans. On Micr. Theory and Tech., vol. 22, pp. 282-288, Mar. 1974.
8. "VectorStar MS464xB Calibration and Measurement Guide," Anritsu Company manual, document 10410-00318B, Oct. 2013.

9. S. Seo, T. Stintzing, I. Block, D. Pavlidis, M. Rieke, and P. Layer, “High frequency wideband permittivity measurements of biological substances using coplanar waveguides and application to cell suspensions,” IEEE MTT-S 2012 Int. Micr. Symp. Dig, June 2012.
10. W. J. Ellison, “Permittivity of pure water, at standard atmospheric pressure, over the frequency range 0-25 THz and the temperature range 0-100C,” J. Phys. Chem. Ref. Data, vol. 36, pp. 1-25 , Feb. 2007.
11. “Calculating VNA measurement accuracy,” Anritsu Company Application note, document number 11410-00464, Dec. 2008.
12. S. Jenkins, A. G. P. Warham, and R. N. Clarke, “Use of open-ended coaxial line sensor with laminar or liquid dielectric backed by a conducting plane,” IEE Proc., vol. 139, pp. 179-182, April 1992.
13. J.-H. Jung and S.-Y. Kim, “Complex permittivity of thin PCB substrate measured by open-ended coaxial probe,” Proc. ISAP 2005, pp. 797-800, 2005.
14. Y. Y. Lim, M. D. Rotaru, A. Alpones, and A. P. Popov, “Simple and improved dielectric parameter extraction of thin organic packaging materials using open-ended coaxial line technique,” IEE Proc. Micr. Antenna Prop., vol. 152, pp. 214-220, Aug. 2005.
15. A. Eriksson, P. Linner, and S. Gevorgian, “Mode chart of electrically thin parallel-plate circular resonators,” IEE Proc. Micr. Antenna Prop., vol. 143, pp. 51-55, Feb. 2001.

11410-0826, Rev. A Printed in United States 2014-09